Functional Materials 16, No.4 (2009)

The thermal expansion of single-walled carbon nanotubes at low temperatures

A.V.Dolbin

B.Verkin Institute for Low Temperature Physics & Engineering, National Academy of Sciences of Ukraine, 61103 Kharkiv, Ukraine

Received August 27, 2009

The radial thermal expansion coefficient α_r of pure and Xe-saturated bundles of single-walled carbon nanotubes has been measured in the interval 2.2–120 K. The coefficient is positive above T = 5.5 K and negative at lower temperatures. The sample was prepared by compacting a CNT powder such that the pressure applied oriented the nanotube axes perpendicular to the axis of the cylindrical sample. The data show that individual nanotubes have a negative thermal expansion coefficient while the solid compacted material has a positive one due to expansion of the intertube volume in the bundles. Doping the nanotubes with Xe caused a sharp increase in α_r in the whole temperature range used, and a peak in the dependence $\alpha_r(T)$ in the 50–65 K interval. A subsequent decrease in the Xe concentration lowered the peak considerably but had a little effect on the thermal expansion coefficient of the sample outside the peak region. The features revealed have been explained qualitatively.

В интервале температур 2,2–120 К измерены коэффициенты радиального теплового расширения α_r чистых и насыщенных ксеноном жгутов одностенных углеродных нанотрубок. Значения α_r положительны выше 5,5 К и отрицательны при более низких температурах. Исследованный образец получен прессованием порошка нанотрубок, в результате которого оси нанотрубок были ориентированы перпендикулярно оси образца. Полученные результаты позволяют предположить, что значения α_r индивидуальных нанотрубок отрицательны, тогда как для объемного образца, ввиду вклада жгутов нанотрубок, α_r положительны. Допирование нанотрубок ксеноном привело к резкому увеличению абсолютных значений α_r во всем исследованном интервале температур, а также к возникновению пика на зависимости $\alpha_r(T)$ в температурном интервале 50–65 К. Последующее уменьшение концентрации примеси ксенона привело к существенному снижению величины пика, однако практически не повлияло на значения коэффициента теплового расширения образца вне области пика. Предложено качественное объяснение обнаруженных особенностей.

Since the discovery of carbon nanotubes (CNTs) in 1991 [1], this novel class of physical objects has been stimulating intense experimental and theoretical research activities. The diversity of CNT types and the problems encountered in obtaining pure CNT material in quantities needed for experimental investigations make it rather difficult to trace the basic trends in the behavior of carbon nanotubes (e.g., see [2] and References therein). Thermal expansion is among the least studied properties of CNTs. The currently available experimental data on the thermal expansion of single-walled nanotubes (SWNTs) and their bundles is confined to the region near and above room temperature, whereas it is just the low temperature data that are of most importance in understanding the CNT dynamics. The theoretically estimated thermal expansion coefficients (TEC) of SWNTs [4–9] vary appreciably both in value and sign.

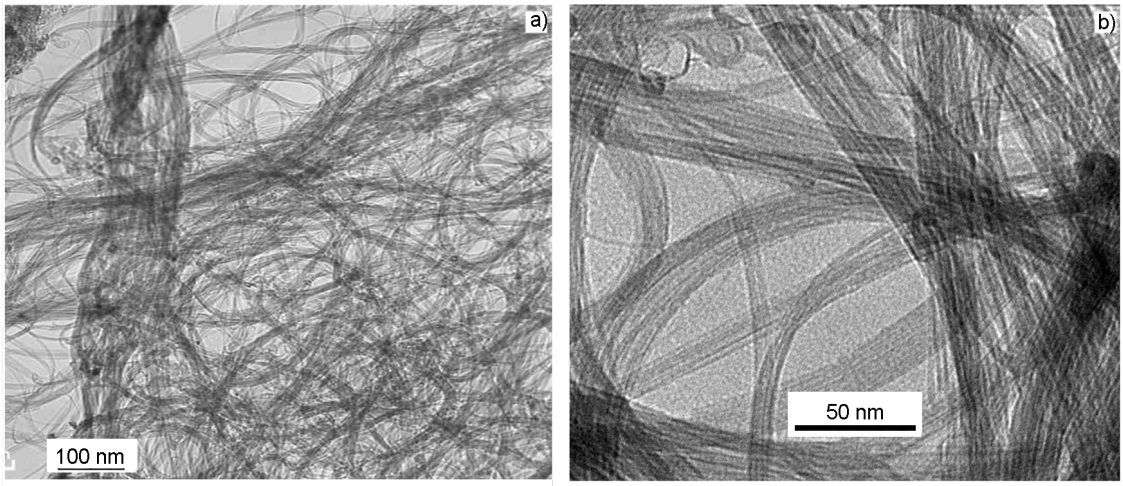

Fig. 1. TEM images of the starting SWNT powder.

Due to their unique geometry, CNTs may provide a basis for novel low-dimensional systems. For example, bundles can be used as templates to form one-dimensional chains or two-dimensional surfaces consisting of condensed impurity molecules.

Recently, much experimental effort has been devoted to the study of structural and thermal properties of such systems and a number of theoretical models have been proposed to predict these properties [10–23]. However, the thermal expansion behavior of SWNT/gas impurity systems still remains obscure. In this study, the radial thermal expansion was measured on a sample consisting of bundles of single-walled nanotubes closed at the ends in the T = 2.2–120 K range and on bundles of SWNTs saturated with Xe at T = 2.2–75 K. The sorption properties of bundled-up SWNTs with closed (c-SWNT) and open (o-SWNT) ends have been studied using the thermally-programmed desorption technique described below.

The sample for thermal expansion measurements was prepared using a procedure for ordering the SWNT axes by applying a pressure of 1 GPa, as described by Bendiab et al. [24]. These authors have shown that in SWNT plates of up to 0.4 mm thickness, such a pressure aligned the CNT axes such that their average angular deviation from a plane normal to the pressure vector is about 4°. The starting material was a CNT powder (CCVD method, Cheap Tubes, USA) which, according to the manufacturer data, contained over 90 % of SWNTs. The main characteristics are presented in Table.

The powder quality was confirmed by Raman analysis performed both by the supplying company and at Umea University, Sweden. According to the manufacturer, the average outer diameter of the tubes was 1.1 nm but no information is available about the chirality distribution. According to our own Raman data obtained using four different excitation lasers with wavelengths in the range 541–830 nm, the radial breathing modes indicate a wide range of tube diameters, 0.8 to 2.1 nm. All samples studied show typical SWNT G-bands and only weak disorder bands. Although multi-wall tubes may also be present, judging from the spread in diameters, the Raman spectra are completely dominated by the response from single (or possibly few-) wall nanotubes. However, a small fraction of MWNTs might be invisible due to their large diameters and possibly lower Raman cross sections.

Table. Characteristics of carbon nanotube powder (the manufacturer data)

Diameter	1–2 nm
Length	5–30 μm
SWNT fraction	> 90 wt. %
Amorphous carbon fraction	< 1.5 wt. %
Co catalyst fraction	2.9 wt. %
Specific surface	> 407 m^2/g
Electrical conduction	> 102 S/cm

The starting SWNT powder was also investigated by high-resolution transmission electron microscopy (HRTEM) at both the Institute of Problems of Materials Science, NAS of Ukraine (Fig. 1a) and at Umea University, Sweden (Fig. 1b). The pictures show that large sample fractions contain some amorphous carbon or residual catalyst. By measuring the bundle diameters, we esti-

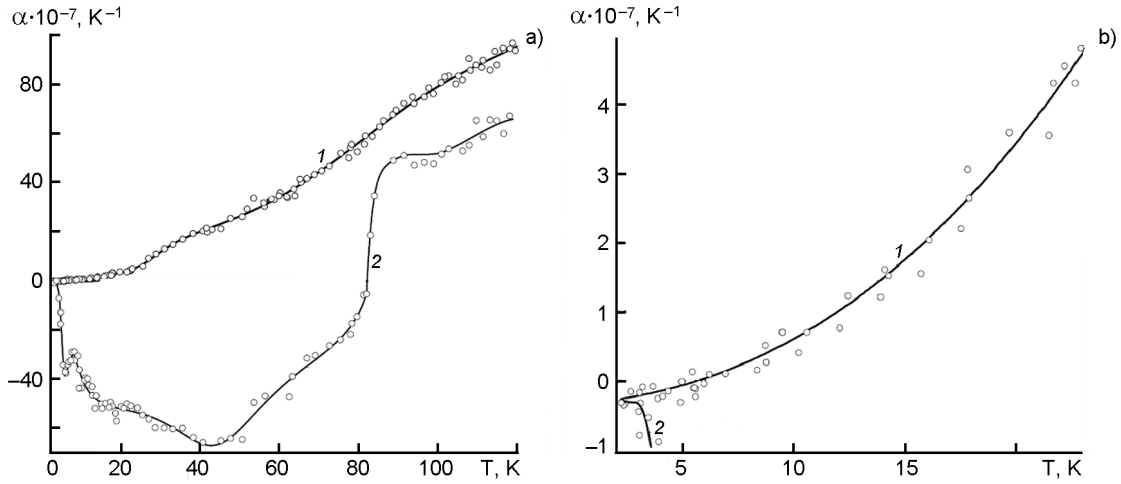

Fig. 2. LTECs of pressure-oriented SWNT compacted sample in the direction perpendicular to the SWNT bundle axes: a) T = 2.2–120 K; b) T = 2.2–25 K (curve *1* — heating and cooling, curve *2* — first heating from T = 2.2 K).

mate that each bundle in the starting powder contains 7 to 600 SWNTs.

The compacted sample used was prepared at Umea University (Sweden) by first compacting the pressure-oriented (P = 1.1 GPa) SWNT plates (an individual plate was up to 0.4 mm thick), then pressing several stacked plates together at a ten per cent higher pressure to form a 7.2 mm high cylinder of 10 mm in diameter with 1.2 g/cm^3 density. The sample was made in a special cylindrical segmented die designed for compacting CNT powder under effective pressures of 0.5 to 2 GPa, consisting of a ring with a cylindrical channel and a conical outer surface, which was inserted into a hardened-steel cylinder supported inside a larger pressure vessel. The structure so arranged was resistant to internal stresses. The 10 mm diameter plunger was made from sintered tungsten carbide (WC). The pressures used were high enough to consolidate the powder into a solid with well oriented tubes [24], but still low enough to keep the integrity and structure of tubes and avoid tube collapse, and Raman spectra taken on pressed plates showed no systematic changes relative to those of the initial powder. The sample prepared by this technology has a pronounced anisotropy of properties in the directions perpendicular and parallel to the sample axis. In the direction perpendicular to the applied pressure, the axes of the SWNT bundles are disordered. The compaction aligns the axes of the SWNT bundles in the plane perpendicular to the sample axis [24]. As a result, the radial expansion component of the SWNT bundles makes a dominant contribution to the sample thermal expansion in the direction parallel to the sample axis. If the axial component of the thermal expansion coefficient is comparable to that of the radial one, an angle of about 4° implies that the typical contribution to the total coefficient from the axial component is about 7 % of the radial component value.

The radial thermal expansion of the sample was studied using a capacitance dilatometer (its design and the measurement technique are described in [25]). The linear thermal expansion coefficient (LTEC) was measured in the direction of the applied compacting pressure, i.e. radially to the SWNT bundles. Prior to measurement, the gas impurities were removed from the sample by dynamic evacuation for 72 h at 10^{-3} Torr and room temperature. Immediately before dilatometric investigation, the measuring cell with the sample was cooled slowly (for 8 h) down to liquid helium temperature (4.2 K) and the sample was held at this temperature for about 4 h. The cooling and examinations were made in vacuum of at least 10^{-5} Torr.

The LTEC temperature dependence in the 2.2–120 K interval is shown in Fig. 2. The curves were obtained by least-square averaging over several series of measurement. The curve *2* was taken during the first heating of the sample from T = 2.2 K. The curve *1* data were measured in the subsequent heating-cooling process. The non-equilibrium LTEC values obtained at the first heating from T = 2.2 K may be connected with the heating-induced alignment and ordering of the bundles and the nanotubes therein, which causes a compression of

bundles and, as a result, negative thermal expansion. The equilibrium radial LTEC α_r (curve *1*) is positive above 5.5 K and negative at lower temperatures.

Assuming that the impurity effect is negligible, α_r comprises two components α_d and α_g caused by temperature-induced changes in the CNT diameters and the intertube gap. Proceeding from a simple Gruneisen-type model, it might be expected that α_d should be similar to the in-plane thermal expansion of graphite, and thus probably small and negative well below room temperature. As the sample is a mixture of all chiralities, the average α_d should also be very similar to the average axial expansion coefficient of the tubes. The thermal expansion of a bundle should thus probably be dominated by α_g, which should be similar to the out-of-plane thermal expansion of graphite or, considering the curvature, to the thermal expansion of fullerenes or linear fullerene polymers [26].

So far, there has been only one study [27] where both α_d and α_g were measured by the X-ray diffraction method in the 300 to 950 K range. At T = 300 K, $\alpha_r = (0.75\pm0.25)\cdot10^{-5}$ K^{-1}, $\alpha_d = (-0.15\pm0.2)\cdot10^{-5}$ K^{-1}, and $\alpha_g = (4.2\pm 1.4)\cdot10^{-5}$ K^{-1}. Another measurement, of α_r only, by the same method [28] resulted in negative values in the whole measurement temperature range (200 to 1600 K). We are not aware of further experimental attempts to directly investigate the thermal expansion of SWNT bundles, but some experiments have been made to estimate the thermal expansion from the temperature dependence of the radial breathing Raman modes of nanotubes. Although these modes shift down rapidly with rising temperature, indicating a large strong positive thermal expansion coefficient, it was concluded by Raravikar et al. [7] that this effect is almost completely caused by changes in intra- and intertube interactions, and that α_d is very small.

It is rather problematic to compare our results with theoretical data quantitatively, mainly because the available theoretical studies are concerned with the radial and axial thermal expansion of individual CNTs only. Some works offer only general conjectures on how thermal expansion can be affected by the interaction of nanotubes in a bundle (e.g., see [8]). Also, there is a poor agreement between theoretical conclusions from different works on the TEC magnitude, sign and temperature dependence, the effect of chirality and CNT diameter on thermal expansion, and on correlation between the radial and axial thermal expansion components for nanotubes. For example, the thermal expansion is negative in a wide temperature interval (0–800 K) in [4], changes from negative values at low temperatures to positive ones at moderate and high temperatures in [8], or is positive at all the temperatures investigated in [6].

The qualitative interpretation of our results is based on the Gruneisen coefficients calculated [8] for carbon modifications — diamond, graphene, graphite and nanotubes. It is found [8] that the Gruneisen coefficients and the radial thermal expansion of CNTs are negative at relatively low temperatures, an effect caused mainly by the contribution from transverse acoustic vibrations perpendicular to the CNT surface. However, our measurements show that a negative thermal expansion coefficient exists only in a temperature interval much more narrow than found in the calculations [8]. We believe that the main reason for this is that the calculations were performed for individual nanotubes only [8]. Our sample is clearly dominated by CNT bundles (Fig. 1), and in this case, additional factors contributing to the thermal expansion come into play. First, there appears a positive contribution α_g caused by variations of the intertube gaps with temperature. Secondly, the nanotube interaction in the bundles suppresses the negative contribution of the transverse acoustic vibrations perpendicular to the nanotube surfaces [8]. These two positive contributions to the thermal expansion of SWNT bundles decrease both the magnitude and the temperature region of the total negative thermal expansion. If we use this model and assume α_d to vary slowly with temperature over a wide temperature interval, we can use the data shown in Fig. 2b to estimate $\alpha_d = (-4\pm1)\cdot 10^{-8}$ K^{-1} at T = 2.2 K. Assuming further that the temperature-dependent part of α at low temperatures is dominated by a positive coefficient α_g, we see from Fig. 2b that a polynomial of the third order in T is a good approximation to $\alpha_g(T)$ up to about 25 K.

Although the data scatter is rather high, it is clear that to get a good fit, it is necessary to include one term in T^3 and one term linear (or, with a less good fit, quadratic) in T. In the Gruneisen model, the thermal expansion coefficient of a bundle is closely related to its specific heat capacity, and it is well known that the experimentally found

low-temperature specific heat of nanotube bundles shows a similar behavior above 2 K [29]. In that case, the experimental behavior $c_p(T) = aT + bT^3$ could be fitted by an anisotropic two-band Debye model at weak coupling between tubes in the bundle by adding a contribution from the first optic branch. It thus seems quite reasonable to attribute the strongly temperature-depending positive component of the total thermal expansion to α_g. The data in Fig. 2a also show a noticeable plateau-like structure between 40 and 60 K. We point out that the intermolecular interaction in C_{60}, which should be similar in magnitude to the intertube interaction, corresponds to an effective Debye temperature near 50–60 K which gives rise to a plateau in the specific heat in this range for both molecular and polymeric C_{60} [30]. The plateau structure observed here might thus indicate the crossover between the acoustic modes and the lowest optical/molecular 3D modes in the bundle lattice.

Carbon nanotubes (CNT) prepared by standard methods (electric-arc, laser evaporation of carbon, or CCVD method) are arranged into bundles. Inside a bundle, the CNTs form a close-packed two-dimensional (2D) triangular lattice [31]. Normally, CNTs have fullerene-like semispheres at the ends (CNTs with closed ends, or c-SWNT). The final CNT product can contain large amounts of amorphous carbon, fullerenes, and other carbon modifications [2, 31–37]. The currently used methods of cleaning CNT materials involve oxidative treatment with acid-oxidant mixtures, ozone [38], etc. Those cause a partial or complete opening of the CNT ends and produce defects at the lateral surfaces. The possible sites for sorption of gas impurity molecules in bundles of infinite, open and equal-diameter SWNTs are shown in Fig. 3. However, in practice, such SWNT systems may include additional zones of impurity sorption. For example, nanotubes of different diameters form rather large channels parallel to the nanotube axes, which can be occupied by impurity molecules [39]. Besides, oxidation can produce interstices between the nanotubes in a bundle [18].

We investigated Xe sorption in c-SWNT and o-SWNT powders at T = 78–200 K. The choice of the temperature interval and the impurity was dictated by the following considerations. The interaction of gas impurities with different parts of the CNT surface is most evident at low temperatures. Owing

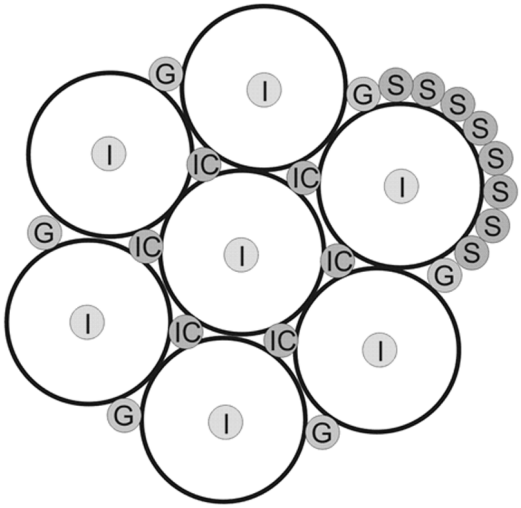

Fig. 3. Possible sorption sites of gas impurity molecules in bundles of infinite, open and equal-diameter SWNTs.

to their geometric configuration, the SWNT bundles ideally (Fig. 3) have preferable sites where sorption of impurity molecules is energy-favorable. A number of theoretical models were proposed [39–43] to describe the physical sorption and dynamics of impurity gas molecules at the surface and in the interstitial channels of SWNT bundles. According to mathematical simulations [43], the inner CNT surfaces and the interstices between the neighboring tubes at the surface of SWNT bundles (the grooves — G, Fig. 3) are the most energy-favorable sites for sorbing the impurity gas molecules. Xe was used because the SWNT/Xe system is already a well-studied "model" system [44–47]. A Xe atom is too large to penetrate into the interstitial channels (IC) of close-packed bundles of identical nanotubes having the binding energy to impurity molecules comparable to that at the inner surface [20]. Therefore, the Xe impurity is sorbed inside a nanotube (I), in a groove between two neighboring tubes at the outer surface of a bundle (G), and at the surface of the individual tubes forming the outer surface of a bundle (S) (see Fig. 3). To obtain the information on the gas impurity desorption from CNT materials, a laboratory test setup was constructed to study the Xe sorption and desorption process in a CNT powder at T = 78–200 K.

The sorption properties of the starting pure c-SWNT powder (0.0416 g) were examined by thermo-programmed desorption. Fig. 4 illustrates the temperature distribution of the desorbed impurity. The greatest

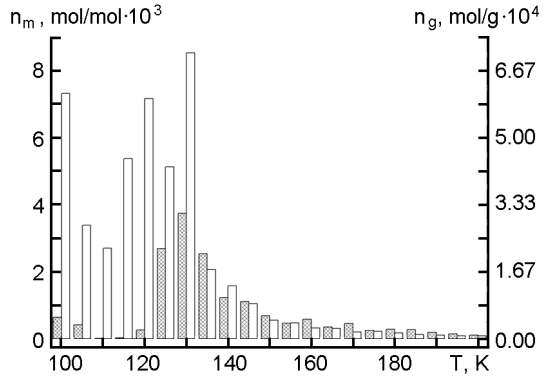

Fig. 4. Temperature distribution of Xe impurity (mole per mole and mole per gram) desorbed from powder samples of c-SWNTs (dark columns) and o-SWNTs (light columns).

amounts of Xe were desorbed at $T = 125$–135 K. In the case of close-packed bundles of infinite equal-diameter SWNTs (Fig. 3), the highest desorption of Xe in this temperature interval is expected from the grooves at the outer bundle surface (*G*) and from the interior channels of some nanotubes (*I*), because Xe atoms have the highest and nearly equal binding energies at these sites [47]. In our powder, the desorption can be enhanced considerably by removal of Xe atoms out of the axial large-diameter channels (IC). Such channels are possible in bundles of nanotubes of varying diameters. Xenon can penetrate into interior channels through defects at the ends or the lateral surfaces that can be present in some nanotubes of the starting powder. A rather small amount of Xe was also desorbed at $T = 100$–105 K, which may be due to removal of the layers (*S*) of Xe molecules formed at the outer surface of SWNT bundles.

To open the nanotube ends, a portion (0.0705 g) of the starting powder was placed into a capsule which was evacuated for 8 h and then heated to 450°C. At this temperature, the capsule was filled with air for 12 min under atmospheric pressure. According to literature data, the ends of over 90 % of CNTs must be opened through this procedure [48]. Thereafter, the capsule was evacuated again to about 10^{-3} Torr, heated to 750°C and held at this temperature for an hour to remove the gaseous oxidation products. The post-treatment weighing has shown a powder mass loss of about 5 %. The sorption properties of the nanotubes with opened ends were then examined using the same thermo-programmed desorption technique. The oxidation-induced opening of the CNT ends made the inner CNT surfaces and the intertube interstices in the bundles accessible to Xe sorption [18], which enhanced the SWNT powder sorption capacity almost fivefold as compared to the starting material (see Fig. 4).

The radial thermal expansion of Xe-saturated SWNTs was studied on the compacted sample used previously to measure the LTECs of pure SWNTs. Immediately before measurement, the cell with a pure CNT sample was evacuated at room temperature for 96 h and then filled with Xe at 760 Torr. The evacuated measuring cell of the dilatometer with the sample in the Xe atmosphere was cooled to 90 K. At this temperature, it was evacuated again and then cooled to liquid helium temperature. The thermal expansion was measured in vacuum down to $1 \cdot 10^{-5}$ Torr.

The temperature dependence of LTEC for a Xe-SWNT sample in the interval 2.2–75 K is shown in Fig. 5 (curve *1*). The sharp increase in LTEC values of the Xe-saturated sample (cf. curves 1, 3) can reasonably be attributed to the heavy Xe atoms affecting the transverse vibrations of the nanotubes in the direction perpendicular to their surface. At low temperatures, the Gruneisen coefficients of such vibrations are negative in two-dimensional (graphene) or quasi-two-dimensional (graphite, nanotubes) carbon systems [8, 49] and positive in a three-dimensional carbon modification (diamond). The formation of SWNT bundles and the sorption of impurity atoms at the surface or inside the nanotubes generate three-dimensional features in the system. As a result, the negative Gruneisen coefficients of such system decrease in magnitude or become positive. The thermal expansion coefficients are expected to behave in a similar way. That is why the negative contribution to the radial thermal expansion of Xe-saturated SWNT bundles decreases and shifts towards lower temperatures (see Fig. 5; cf. curves *1*, *2* and *3*).

In contrast to pure CNTs, the thermal expansion of Xe-saturated SWNTs is similar during the first heating and in the subsequent heating and cooling runs. It is possible that the first heating of pure SWNT bundles with xenon can make the system more rigid and its geometry insensitive to heating at low temperatures.

It is interesting that the LTECs have maximum values in the interval 50–65 K, which may be a manifestation of spatial redistribution of Xe atoms in the SWNT bun-

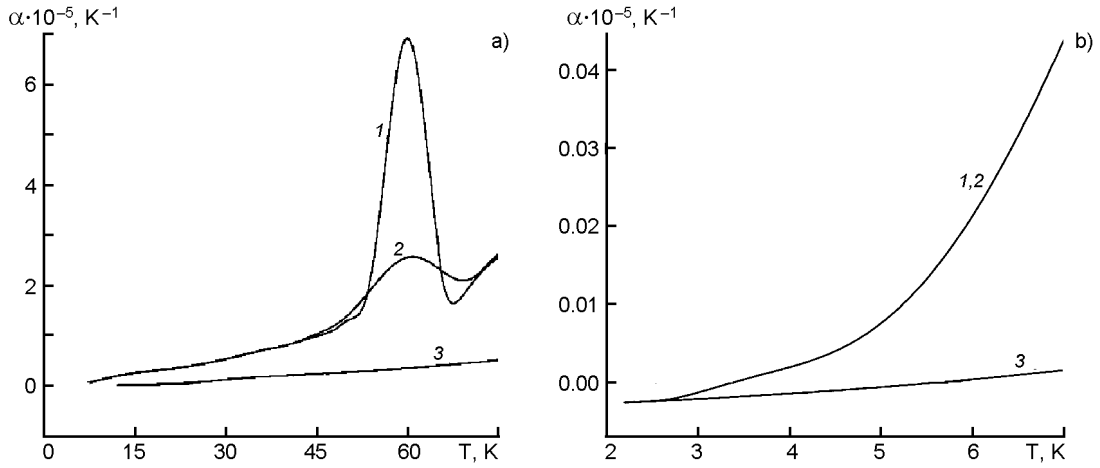

Fig. 5. The radial LTECs of SWNT bundles: *1*, Xe-saturated bundles; *2*, after partial Xe removal at T = 110 K; *3*, pure SWNTs (α_r) at T = 2.2–75 K (a) and 2.2–7 K (b), compacted sample.

dles. The potential energy simulation (by Wang-Landau algorithm) [23, 50] for a system of SWNT bundles saturated with inert gases predicted peaks in the temperature dependence of the heat capacity at T = 50–100 K, attributed to reordering of the impurity atoms.

To test the prediction, it was necessary to remove the Xe impurity from the surface of the SWNT bundles. To that end, the sample was heated to T = 110 K. This temperature causes an intensive Xe desorption from the sample surface but leaves it undisturbed in the grooves of the SWNT bundles (G) and the inner interstices (I) of the nanotubes having surface defects (Fig. 4). The sample was kept at T = 110 K until the desorbed Xe was completely removed and the pressure in the measuring cell reached ~ $1 \cdot 10^{-5}$ Torr. The sample was then cooled to T = 2.2 K and the thermal expansion was measured again (Fig. 5, curve *2*). It is seen that the LTEC peak is much lower after Xe was removed from the SWNT bundle surfaces. However, this partial Xe desorption leaves the temperature dependence of the LTEC practically unaffected outside the interval of the peak. This suggests that the Xe atoms localized at the bundle surface affect only slightly the thermal expansion of SWNT bundles when the process of spatial redistribution of atoms are absent.

In conclusion, temperature dependences of the radial thermal expansion coefficients $\alpha_r(T)$ for pure and Xe-saturated SWNT bundles at low temperatures have been studied experimentally for the first time. The measurements were made on heating and cooling the samples in the interval 2.2–120 K using a capacitance dilatometer. The dependence $\alpha_r(T)$ measured on the first heating shows a very strong nonequilibrium effects, and in the interval 3.2–120 K it differs significantly from the well reproducible equilibrium dependences $\alpha_r(T)$ measured at subsequent heating and cooling runs. The equilibrium radial thermal expansion coefficients α_r (Fig. 2, curve *1*) are positive above 5.5 K and negative at lower temperatures. The nonequilibrium radial thermal expansion coefficients α_r (Fig. 2, curve *2*) are negative in the interval 2.2–82 K. It is assumed that the non-equilibrium α_r-values measured at the first heating of the sample are due to the irreversible alignment and ordering of the bundle positions and the nanotubes in the bundles at rising temperature. As this occurs, the system density increases, so the thermal expansion becomes negative.

The qualitative interpretation of the equilibrium dependence $\alpha_r(T)$ is based on the theoretical conclusions about the Gruneisen coefficients for carbon modifications [8]. The Gruneisen coefficient and the radial thermal expansion of nanotubes are negative at reasonably low temperatures [8], what is defined mainly by the contribution of the transverse acoustic vibrations perpendicular to the nanotube surfaces. However, in the experiment, the temperature interval of the negative thermal expansion is much narrower in comparison with the theoretical predictions. This is most likely because the cited theory [8] considered individual nanotubes. Additional contributions to the thermal expansion come into play in SWNT bundles. First, there is a positive contribution α_g, caused by vari-

ations of the intertube gaps with temperature. In addition, the nanotube interaction in the bundles suppresses the negative contribution from the transverse acoustic vibrations perpendicular to the nanotube surfaces [8]. These two positive contributions to thermal expansion of the SWNT bundles decrease both the magnitude and the temperature interval of the negative thermal expansion.

The saturation of SWNT bundles with xenon brings about new features in their thermal expansion. First, the α_r value increases sharply in the whole temperature range being investigated. This is because the Xe impurity suppresses the negative contribution to the thermal expansion from the transverse acoustic vibrations perpendicular to the nanotube surfaces [8]. Second, the dependence $\alpha_r(T)$ has a peak in the 50–65 K interval, which appears to be due to the spatial redistribution of the Xe atoms over the SWNT bundle surfaces. The removal of Xe impurity from these surfaces decreases the peak significantly but leaves the temperature dependence of the LTEC practically unchanged outside the interval of the peak. This suggests that the Xe atoms located at the bundle surfaces effect weakly the thermal expansion of SWNT bundles when the processes of their spatial redistribution are absent. Third, for the Xe saturated material, there is no non-equilibrium thermal expansion behavior such as was observed during the first heating of the sample and attributed to irreversible alignment and ordering of the bundle positions and nanotubes in the bundles at rising temperature. Perhaps the saturation with Xe makes the system of SWNT bundles more rigid and its geometry insensitive to heating in a low temperature interval.

Finally, the employed thermoprogrammed desorption technique has made it possible to measure the temperature dependence of Xe desorption from both open and closed SWNT bundles.

The author is thankful to Science Technology Center in Ukraine for the financial sapport of this study (project №4266)

References

1. S.Iijima, *Nature*, **354**, 56 (1991).
2. A.V.Eletskii, *Phys. Usp.*, **47**, 1119 (2004).
3. H.Jiang, B.Liu, Y.Huang, *J. Eng. Mater. Technol.*, **126**, 265 (2004).
4. Y.Kwon, S.Berber, D.Tomanek, *Phys. Rev. Lett.*, **92**, 015901 (2004).
5. N.M.Prakash, Determination of Coefficient of Thermal Expansion of Single-walled Carbon Nanotubes Using Molecular Dynamics Simulation, The Florida State University, Master of Science Thesis (2005), p.54.
6. C.Li, T.Chou, *Phys. Rev. B*, **71**, 235414 (2005).
7. N.R.Raravikar, P.Keblinski, A.M.Rao et al., *Phys. Rev. B*, **66**, 235424 (2002).
8. P.K.Schelling, P.Keblinski, *Phys. Rev. B*, **68**, 035425 (2003).
9. G.Cao, X.Chen, J.W.Kysar, *Phys. Rev. B*, **72**, 235404 (2005).
10. B.K.Pradhan, A.R.Harutyunyan, D.Stojkovic et al., *J. Mater. Res.*, **17**, 2209 (2002).
11. M.R.Johnson, S.Rols, P.Wass et al., *Chem. Phys.*, **293**, 217 (2003).
12. S.Ramachandran, T.A.Wilson, D.Vandervelde et al., *J. Low Temp. Phys.*, **134**, 115 (2004).
13. Y.H.Kahng, R.B.Hallock, E.Dujardin, *Physica B: Cond. Matter*, **329**, 280 (2003).
14. T.Wilson, A.Tyburski, M.R.DePies et al., *J. Low Temp. Phys.*, **126**, 403 (2002).
15. F.R.Hung, K.E.Gubbins, R.Radhakrishnan et al., *Appl. Phys. Lett.*, **86**, 103110 (2005).
16. H.Chen, J.K.Johnson, D.S.Sholl, *J. Phys. Chem. B*, **110**, 1971 (2006).
17. C.Matranga, L.Chen, B.Bockrath, J.K.Johnson, *Phys. Rev. B*, **70**, 165416 (2004).
18. A.Kuznetsova, J.T.J.Yates, V.V.Simonyan et al., *J. Chem. Phys.*, **115**, 6691 (2001).
19. Adsorption by Carbons, Eds. E.Bottani and J.Tascon, Elsevier, Amsterdam (2008).
20. D.G.Narehood, J.V.Pearce, P.C.Eklund et al., *Phys. Rev. B*, **67**, 205409 (2003).
21. S.M.Gatica, M.J.Bojan, G.Stan et al., *J. Chem. Phys.*, **114**, 3765 (2001).
22. M.M.Calbi, S.M.Gatica, M.J.Bojan et al., *J. Chem. Phys.*, **115**, 9975 (2001).
23. N.M.Urban, S.M.Gatica, M.W.Cole, J.L.Riccardo, *Phys. Rev. B*, **71**, 245410 (2005).
24. N.Bendiab, R.Almairac, J.Sauvajol, S.Rols, *J. Appl. Phys.*, **93**, 1769 (2002).
25. A.N.Aleksandrovskii, V.B.Esel'son, V.G.Manzhelii et al., *Fiz. Nizk. Temp.*, **23**, 1256 (1997) [*Low Temp. Phys.*, **23**, 943 (1997)].
26. P.Nagel, V.Pasler, S.Lebedkin et al., *Phys. Rev. B*, **60**, 16920 (1999).
27. Y.Maniwa, R.Fujiwara, H.Kira et al., *Phys. Rev. B*, **64**, 241402 (2001).
28. Y.Yosida, *J. Appl. Phys.*, **87**, 3338 (2000).
29. J.Hone, B.Batlogg, Z.Benes et al., *Science*, **289**, 1730 (2000).
30. A.Inaba, T.Matsuo, A.Fransson, B.Sundqvist, *J. Chem. Phys.*, **110**, 12226 (1999).
31. A.Thess, R.Lee, P.Nikolaev et al., *Science*, **273**, 483 (1996).
32. A.G.Rinzler, J.Liu, H.Dai et al., *Appl. Phys. A*, **67**, 29 (1998).
33. A.C.Dillon, T.Gennett, K.M.Jones et al., *Adv. Mater.*, **11**, 1354 (1999).
34. A.V.Eletskii, B.M.Smirnov, *Usp. Fiz. Nauk*, **163**, 33 (1993).

35. A.V.Eletskii, B.M.Smirnov, *Phys. Usp.*, **38**, 935 (1995).
36. A.V.Eletskii, *Phys. Usp.*, **40**, 899 (1997).
37. B.P.Tarasov, N.F.Goldshleger, A.P.Moravsky, *Russ. Chem. Rev.*, **70**, 131 (2001).
38. D.B.Mawhinney, V.Naumenko, A.Kuznetsova et al., *J. Am. Chem. Soc.*, **122**, 2383 (2000).
39. W.Shi, J.K.Johnson, *Phys. Rev. Lett.*, **91**, 015504 (2003).
40. M.W.Cole, V.H.Crespi, G.Stan et al., *Phys. Rev. Lett.*, **84**, 3883 (2000).
41. M.T.Cvitas, A.Siber, *Phys. Rev. B*, **67**, 193401 (2003).
42. A.Siber, *Phys. Rev. B*, **66**, 235414 (2002).
43. G.Stan, M.Bojan, S.Curtarolo et al., *Phys. Rev. B*, **62**, 2173 (2000).
44. A.Kuznetsova, D.B.Mawhinney, V.Naumenko et al., *Chem. Phys. Lett.*, **321**, 292 (2000).
45. A.Kuznetsova, J.T.J.Yates, J.Liu, R.E.Smalley, *J. Chem. Phys.*, **112**, 9590 (2000).
46. V.V.Simonyan, J.K.Johnson, A.Kuznetsova, J.T.J.Yates, *J. Chem. Phys.*, **114**, 4180 (2001).
47. H.Ulbricht, J.Kriebel, G.Moos, T.Hertel, *Chem. Phys. Lett.*, **363**, 252 (2002).
48. P.M.Ajayan, T.W.Ebbesen, T.Ichihashi, S.Iijima, *Nature*, **362**, 522 (1993).
49. A.C.Bailey, B.Yates, *J. Appl. Phys.*, **41**, 5088 (1970).
50. E.S.Daniel, M.U.Nathan, W.C.Milton, *Phys. Rev. B*, **77**, 205427 (2008).

Теплове розширення джгутів одностінних вуглецевих нанотрубок при низьких температурах

О.В.Долбин

В інтервалі температур 2,2–120 К виміряно коефіцієнти радіального теплового розширення α_r чистих та насичених ксеноном джгутів одностінних вуглецевих нанотрубок. Значення α_r є додатними вище 5,5 К та від'ємними при нижчих температурах. Досліджений зразок одержано пресуванням порошку нанотрубок, в результаті якого осі нанотрубок були орієнтовані перпендикулярно осі зразка. Одержані результати дозволяють припустити, що значення α_r індивідуальних нанотрубок від'ємні, тоді як для об'ємного зразка, внаслідок вкладу джгутів нанотрубок, α_r є додатним. Допування нанотрубок ксеноном спричинило різке збільшення абсолютних значень α_r в усьому інтервалі температур, який досліджено, а також виникнення піка на залежності $\alpha_r(T)$ у температурному інтервалі 50–65 К. Наступне зниження концентрації домішки ксенону спричинило істотне зменшення величини піка, однак практично не вплинуло на значення коефіцієнта теплового розширення зразка поза областю піка. Запропоновано якісне пояснення виявлених особливостей.